Comparison of geomechanical deformation induced by megatonne-scale CO_2 storage at Sleipner, Weyburn, and In Salah

James P. Verdon[a,1], J.-Michael Kendall[a], Anna L. Stork[a], R. Andy Chadwick[b], Don J. White[c], and Rob C. Bissell[d]

[a]School of Earth Sciences, University of Bristol, Bristol BS8 1RJ, UK; [b]British Geological Survey, Keyworth, Nottingham NG12 5GG, UK; [c]Geological Survey of Canada, Ottawa, ON, Canada K1A 0E8; and [d]BP Alternative Energy, Sunbury on Thames, Middlesex TW16 7LN, UK

Edited by Mark H. Thiemens, University of California, San Diego, La Jolla, CA, and approved June 13, 2013 (received for review February 4, 2013)

Geological storage of CO_2 that has been captured at large, point source emitters represents a key potential method for reduction of anthropogenic greenhouse gas emissions. However, this technology will only be viable if it can be guaranteed that injected CO_2 will remain trapped in the subsurface for thousands of years or more. A significant issue for storage security is the geomechanical response of the reservoir. Concerns have been raised that geomechanical deformation induced by CO_2 injection will create or reactivate fracture networks in the sealing caprocks, providing a pathway for CO_2 leakage. In this paper, we examine three large-scale sites where CO_2 is injected at rates of ∼1 megatonne/y or more: Sleipner, Weyburn, and In Salah. We compare and contrast the observed geomechanical behavior of each site, with particular focus on the risks to storage security posed by geomechanical deformation. At Sleipner, the large, high-permeability storage aquifer has experienced little pore pressure increase over 15 y of injection, implying little possibility of geomechanical deformation. At Weyburn, 45 y of oil production has depleted pore pressures before increases associated with CO_2 injection. The long history of the field has led to complicated, sometimes nonintuitive geomechanical deformation. At In Salah, injection into the water leg of a gas reservoir has increased pore pressures, leading to uplift and substantial microseismic activity. The differences in the geomechanical responses of these sites emphasize the need for systematic geomechanical appraisal before injection in any potential storage site.

carbon sequestration | geomechanics | InSAR | microseismic monitoring

Carbon capture and storage (CCS)—where CO_2 is captured at large point source emitters (such as coal-fired power stations) and stored in suitable geological repositories—has been touted as a technology with the potential to achieve dramatic reductions in anthropogenic greenhouse gas emissions (1, 2). However, its success is dependent on the ability of reservoirs to retain CO_2 over long timescales (a minimum of several thousand years). If CCS is to make a significant impact on global emissions, more than 3.5 billion tons of CO_2 per year must be stored (3), which at reservoir conditions will have a volume of ∼30 billion barrels (4).

Secure storage of such large volumes of CO_2 requires more than just the availability of the appropriate volumes of pore space. CO_2 is buoyant in comparison with the saline brines that fill the majority of putative storage sites. Therefore, injected CO_2 will rise through porous rocks and return to the surface, unless trapped by impermeable sealing layers (such as shales and evaporites). Preliminary estimates have tended to indicate that, from a volumetric perspective at least, sufficient storage capacity exists for many decades of CO_2 emissions in deep-lying saline aquifers that have suitable sealing capability (5).

It is equally important that the integrity of the seal is not compromised by injection activities during the life of the storage site. Injection activities can compromise seal integrity in a number of ways: the wellbores themselves may provide a leakage pathway if the cement is compromised by either mechanical or chemical effects (6); chemical reactions between CO_2-saturated brines and the minerals of the caprock might increase caprock permeability, reducing its ability to retain CO_2 (7); and geomechanical deformation induced by pore pressure increases can create or reactivate fracture networks in the caprock that provide a leakage pathway. It is on the geomechanical risks to storage security that this paper is focused.

We note that the highest profile and strongest criticism of CCS derives from considerations of the geomechanical response to CO_2 injection: Zoback and Gorelick (4) directly identify the risks posed to secure storage by geomechanical deformation; similarly, although ostensibly a paper modeling reservoir pore pressure increases during injection, the limiting factor identified by Economides and Ehlig-Economides (8) is that there will be an upper pressure that cannot be exceeded without risking the integrity of the seal by generating fractures.

In this paper, we examine three commercial-scale sites where CO_2 is stored at rates approaching or greater than 1 megatonne (Mt) of CO_2 per y: the Sleipner Field in the Norwegian North Sea (9); the Weyburn Field, Central Canada (10); and the In Salah Field, Algeria (11). These represent three of the most significant commercial-scale CCS projects, although further demonstration projects are likely to commence in the coming decade (12). The amount of geomechanical deformation produced by CO_2 injection is likely to be a function of the volume of CO_2 injected: therefore, it is highly instructive to consider the

Significance

The economic and political viability of carbon capture and sequestration (CCS) is dependent on the secure storage of CO_2 in subsurface geologic reservoirs. A key leakage risk is that posed by geomechanical deformation generating fractures in otherwise sealing caprocks. This study examines this risk, comparing and contrasting deformation induced at three large-scale CCS sites—Sleipner (Norwegian North Sea), Weyburn (Canada), and In Salah (Algeria). These sites show very different geomechanical responses, highlighting the importance of systematic geomechanical appraisal prior to injection, and comprehensive, multifaceted monitoring during injection at any future large-scale CCS operations.

Author contributions: J.P.V. and J.-M.K. designed research; J.P.V., A.L.S., R.A.C., D.J.W., and R.C.B. performed research; J.P.V., A.L.S., R.A.C., and D.J.W. analyzed data; A.L.S. analyzed In Salah microseismic data; R.A.C. analyzed Sleipner pressure performance; D.J.W. analyzed Weyburn microseismic data; R.C.B. modeled fluid flow and geomechanics at In Salah; and J.P.V. wrote the paper.

The authors declare no conflict of interest.

This article is a PNAS Direct Submission.

Freely available online through the PNAS open access option.

[1]To whom correspondence should be addressed. E-mail: james.verdon@bristol.ac.uk.

This article contains supporting information online at www.pnas.org/lookup/suppl/doi:10.1073/pnas.1302156110/-/DCSupplemental.

geomechanical deformation experienced at these large "megatonne" storage sites, as these will inform us of the potential geomechanical issues that will be experienced as commercial-scale, megatonne injection sites are developed in the coming decades.

Geomechanical Response to CO_2 Injection

The effective stress, σ'_{ij}, acting on porous rocks is defined by Terzaghi (13) as follows:

$$\sigma'_{ij} = \sigma_{ij} - \beta_W \delta_{ij} P, \quad [1]$$

where σ_{ij} is the stress applied by regional tectonic stresses and the overburden weight, β_W is the Biot–Willis coefficient, δ_{ij} is the Kroenecker δ, and P is the pore pressure. Therefore, any increase in pore pressure induced by injection will reduce the effective stress, which will in turn lead to inflation of the reservoir. The magnitude of this inflation will be controlled by the magnitude of the pore pressure increase, and the geometry and material properties of the reservoir (14).

As well as directly changing the effective stress acting on reservoir rocks via Eq. **1**, inflation of the reservoir will lead to changes in the applied stress both in and around the reservoir. Small amounts of deformation are common in many settings, and will not pose a risk to storage security. However, if deformation becomes more substantial, it can affect storage operations in a number of ways, illustrated schematically in Fig. 1. The principal risks posed by geomechanical deformation to secure storage are summarized below.

Reservoir Inflation and Alteration of Flow Properties. Pore pressure increase and inflation can influence the flow properties of a storage reservoir. Laboratory experiments show that permeability is sensitive to pressure (15). Furthermore, pore pressure increases may open existing fracture networks in the reservoir, or create new ones, along which CO_2 can flow more rapidly. Permeability increases within the reservoir will not pose a direct leakage risk. Nevertheless, if permeability is increased during injection, this will reduce the accuracy of fluid flow simulations used to predict the resulting CO_2 distribution. The result may be that CO_2 reaches spill-points or breaks through at other wells faster than anticipated, reducing the amount of CO_2 that can be stored. For example, Bissell et al. (16) have shown that injectivity at In Salah is pressure dependent, implying that CO_2 flow is controlled at least in part by the opening and closing of fractures in the reservoir.

Fracturing of Sealing Caprocks. Deformation in a reservoir is generally transferred into the surrounding rocks. This can lead to the creation or reactivation of fracture networks around and above a reservoir. Fractures running through an otherwise impermeable caprock could compromise the storage integrity, providing permeable pathways for CO_2 to escape from the reservoir. This is probably the greatest risk to storage security posed by geomechanical deformation. Leakage of gas through fractured caprock has been observed above hydrocarbon reservoirs (17, 18) and at natural gas storage sites (19).

Triggering of Seismicity. Beginning with the earthquakes triggered by waste fluid injection at the Rocky Mountain Arsenal (20), it has been recognized that subsurface fluid injection is capable of triggering felt (of sufficient magnitude to be felt by nearby populations, so typically $M_L > 2$) seismic events on preexisting tectonic faults (21). Recently, examples of tectonic activity triggered by disposal of waste water from hydraulic fracturing have been noted. Of course, it should be kept in mind that, of thousands of fluid injection wells, only a handful have experienced such seismic events (22). Even if felt seismicity is induced during CO_2 injection, it is unlikely that events would be of sufficient magnitude to damage property or endanger life. Nevertheless, regular triggering of felt seismic events would represent a significant "own-goal" from a public relations and political perspective, and local opposition has already proved to be a significant obstacle to planned CCS projects (23). More significantly, triggering of larger seismic events will indicate that the failure condition on small faults has been met due to anthropogenic pressure changes, with implications for caprock integrity issues as discussed above.

Wellbore Failure and Casing Damage. Geomechanical deformation in producing reservoirs has been observed to cause failure of wellbore casing (24). It is conceivable that either bedding-parallel slip in layers above the reservoir, or expansion of the reservoir against the overburden, could cause shearing of the wellbore. As well as the associated costs, damaged well casing in the overburden presents a significant leakage risk. Although the authors are not presently aware of any incidence of geomechanically induced wellbore failure during CO_2 injection, the risk to storage integrity posed by mechanical effects in the wellbore is an issue that must be considered at future storage sites.

Monitoring Geomechanical Deformation

Fig. 1 also illustrates the variety of methods that can be used to monitor geomechanical deformation in the field. Although the importance of geomechanical deformation in oil production is becoming increasingly appreciated, monitoring it in the field remains something of a niche activity. Nevertheless, a number of

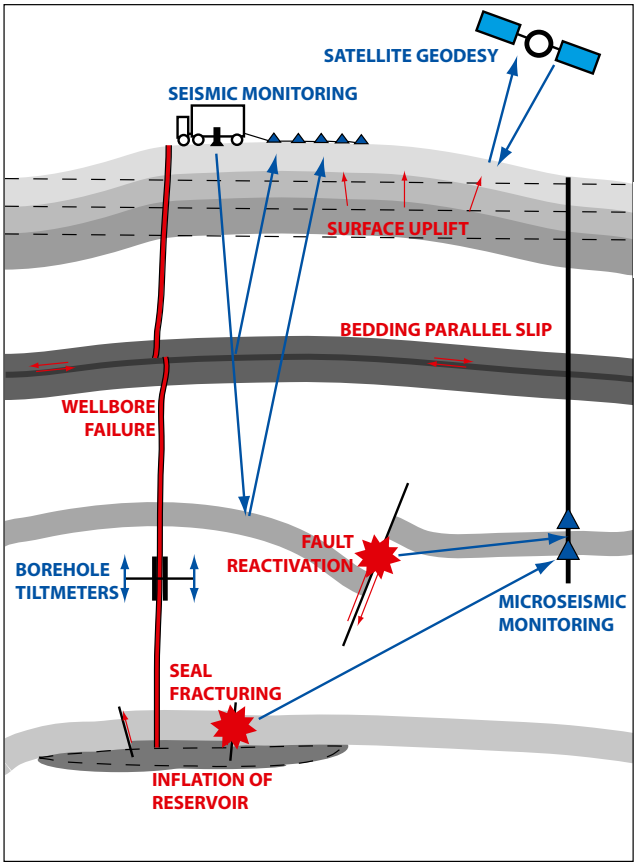

Fig. 1. Schematic illustration showing how geomechanical deformation can influence CO_2 storage sites (red text), and potential monitoring options (blue text). Adapted from Herwanger and Horne (34).

technologies are available to characterize injection-induced deformation.

Geodetic Methods. Is has been observed that deformation in a reservoir can be transferred all of the way to the surface, resulting in uplift or subsidence (25). Geodetic techniques can be used to measure this displacement. In particular, satellite-based Interferometric Synthetic Aperture Radar (InSAR) has been particularly successful in imaging surface displacement in a range of volcanic and tectonic settings (26). InSAR is most effective in bare, rocky settings. In more challenging environments, particularly heavily vegetated or farmed areas, purpose-built reflectors may need to be installed to provide measurement points. An alternative to satellite-based methods (which will be particularly necessary for subsea storage sites) is to install tiltmeters to measure tilting induced by uplift (27). Tiltmeters are typically installed at the surface. However, borehole tiltmeters are also available that can measure deformation at depth (28). Similarly, differential global positioning system measurements can be used to measure the displacement of the ground surface.

Geodetic measurements typically provide a map of displacement of the surface. Numerical modeling techniques must then be applied, using surface displacement as a boundary condition, to invert for processes occurring at depth (29). Often, inversions of this type are nonunique, as a variety of models are capable of accounting for the observed uplift, meaning that such measurements may provide only a broad indication of the deformation processes acting in and around the target reservoir. Similarly, deformation at depth need not produce surface displacement, meaning that a lack of surface displacement alone cannot be taken as a guarantee that deformation of some kind is not occurring at reservoir depths.

Seismic Reflection Surveys. Time-lapse seismic reflection surveys are typically used to image changes in fluid saturation in the reservoir: substitution of CO_2 for the initial brine or oil usually creates a significant reflection contrast at the top of the reservoir, and a time delay for waves traveling through the reservoir (9). Moreover, it has long been known that seismic velocities are also stress sensitive (30). Therefore, accurate time-lapse surveys can also be used to image changes in seismic velocity induced by geomechanical deformation (31, 32). Extension or compaction of the overburden can be imaged by travel time shifts through these areas. Additionally, changes in seismic anisotropy, measured via azimuthal variations in seismic attributes, can be particularly revealing in terms of rotations of stress tensors during deformation (33, 34).

Microseismic Monitoring. The use of microseismic monitoring to image hydrocarbon reservoirs has seen significant expansion in the past decade, fueled mainly by the need to monitor hydraulic fracturing of tight and shale gas reservoirs (35). However, it has also been used to monitor deforming reservoirs (36–38). Although analogous to earthquakes, seismic events triggered during reservoir deformation are usually far smaller (typically M_W is −3–0), so they are commonly known as "microearthquakes" or "microseismic events." The seismic waves emitted by these events can be detected using geophones placed in boreholes near the reservoir (39), or on a dense array of geophones at the surface (40), and the events located using techniques drawn from global seismology. Given that they are caused by injection-induced stress changes, microseismic events represent a tangible manifestation of geomechanical deformation. Furthermore, the seismic waves from microseismic events occurring near the reservoir and recorded on downhole geophones will have traveled only through rocks that are of direct interest to CO_2 storage security. Therefore, wave propagation effects, in particular seismic anisotropy as measured by shear-wave splitting, can also provide useful information about geomechanical deformation around the reservoir (41, 42). Microseismic monitoring is currently benefitting from extensive investment as a tool for monitoring hydraulic fracture stimulation in shale gas reservoirs: the advances made in this field can be readily applied to monitoring injection at CCS sites (43).

Sleipner

Since 1996, CO_2 has been stripped from natural gas produced from the Sleipner Field and reinjected into the overlying Utsira Sand saline aquifer at a rate of ∼1 Mt/year. By late 2011, around 13 Mt had been injected. The Utsira Sand is a very large saline aquifer, with very few barriers to flow: it has an average porosity of 35–40%, permeabilities in the range 1–3 darcys (d); and there is little evidence of any faulting that might serve to compartmentalize the reservoir. There are thin horizontal bands of mudstone within the Utsira that do act as baffles, but these are not laterally continuous. The total pore volume of the Utsira Sand has been estimated at 6×10^{11} m^3 (44), whereas at in situ conditions, the total amount of CO_2 injected by 2011 has a volume of 18×10^6 m^3, meaning that the percentage of the total Utsira pore space filled by CO_2 is ∼0.003% (45). The combination of excellent flow properties, and a very large storage volume, means that pressure changes during CO_2 injection into the Utsira Sand are expected to be negligible.

Chadwick et al. (45) assessed the pressure performance of the Utsira Sand using both wellhead pressure data and time-lapse reflection seismic data. Fig. 2*C* shows the wellhead injection pressures. The elevated pressures during the first months of injection, and from late 2001 to 2003, were caused by technical problems: initially due to sand blocking the perforation screens; and later due to problems with the thermostatic temperature controls. Apart from these anomalous readings, the wellhead

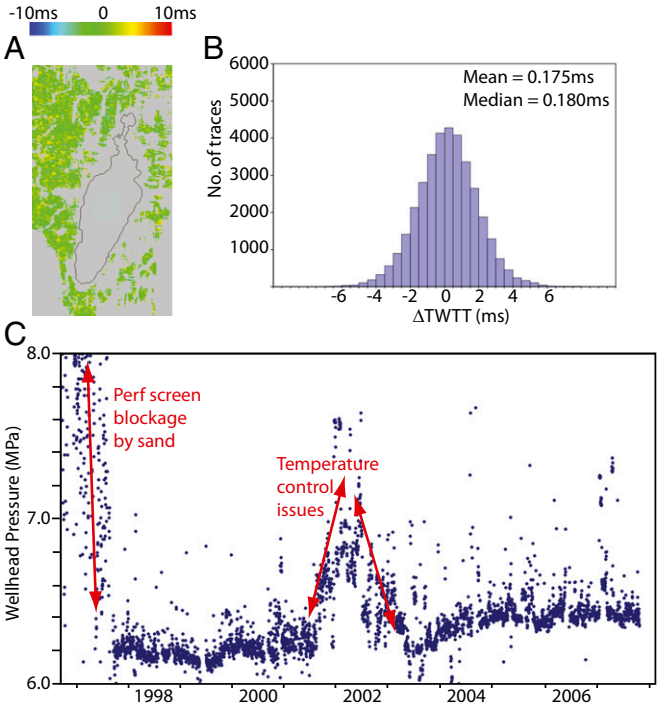

Fig. 2. Pressure performance of the Utsira Sand [based on Chadwick et al. (45)]. *A* shows a map of seismic travel time shifts (1998–2006) through the reservoir outside of the CO_2 plume. *B* shows a histogram of two-way travel time shifts. *C* shows wellhead injection pressures.

pressures have been quite uniform, showing a slight increase during the injection period from 6.2 to 6.4 MPa. This is consistent with only small changes in the reservoir pressure, but because of two-phase (liquid/vapor) behavior of CO_2 in the wellbore (which renders CO_2 density very sensitive to pressure change), reservoir pressure cannot be directly correlated with wellhead pressure.

Chadwick et al. (45) went on to use time-lapse seismic data to estimate pressure increase in the reservoir, on the principle that an increase in pressure reduces seismic velocities and creates a travel time increase through the reservoir. This analysis was performed away from the observed CO_2 plume, where a significant velocity slowdown is caused by substitution of brine for CO_2. Fig. 2*A* shows a map of measured travel time shifts measured outside of the CO_2 plume footprint, and Fig. 2*B* shows a histogram of the same measurements.

The observed scatter in time shifts (Fig. 2*B*) is caused by nonperfect survey repeatability, necessitating a statistical analysis that compares observed travel time distributions with those estimated from simulated pressure increases. This shows that the observed distribution of travel time shifts is consistent with a pore pressure change of significantly less than 0.1 MPa (45). The inversion of velocities for pressure change used a published empirical pressure–velocity relationship for sandstone based on laboratory measurements and supported by a wide range of independent laboratory studies. Nevertheless, there is some evidence that, at the field-scale, velocity sensitivities might be lower than laboratory determinations by a factor of up to 3, depending on lithology (46). Chadwick et al. acknowledged this, but even when they applied the "reduced sensitivity factor" to their calculations they were still able to constrain the maximum pressure increase to only 0.17 MPa.

No direct measurements of geomechanical deformation, either geodetic or microseismic, have been carried out at Sleipner, but with the estimated small pore pressure change, it is unlikely that significant geomechanical deformation will have occurred. However, the question remains—can we find thousands of Sleipners to accommodate the world's CO_2 emissions? If we cannot, we may be forced to use reservoirs where injection does lead to pore pressure increase, and therefore to geomechanical deformation. Therefore, we go on to consider the next megatonne storage site, the Weyburn oilfield.

Weyburn

The Weyburn oilfield, Saskatchewan Province, Canada, is a mature oilfield that has been under production for more than 50 y. Discovered in 1955, production was initially unsupported until 1965, when water injection was initiated for pressure support. In the 1990s, horizontal infill wells were drilled, targeting in particular the lower permeability layers in the reservoir. In 2000, CO_2 injection was initiated. The commercial purpose of CO_2 injection was for enhanced oil recovery. However, a significant research component was added with the expectation of permanently storing over 30 Mt of CO_2 by the end of field operation.

Fig. 3*B* shows a history-matched model of average pore pressures across the phase IB area of the field (this is the region where microseismic monitoring has been conducted). Initially conditions were hydrostatic, with pore pressures at 15 MPa. Between 1955 and 1965, unsupported production reduced pore pressures to 6–7 MPa. From 1965, water injection returned pressures to initial conditions, where they remained relatively stable. From 2000, CO_2 injection has increased pore pressures to 20 MPa. As Weyburn is an enhanced oil recovery field, injection and production is occurring simultaneously, creating pore pressure variations across the field, which are mapped in Fig. 3*A*.

The principal method chosen to monitor geomechanical deformation at Weyburn was to use a microseismic array. A single downhole array of eight three-component geophones was installed in 2003 (47). The monitoring array covers only a small portion of the field: its purpose was to investigate the feasibility of using microseismic monitoring for CCS, rather than to provide comprehensive coverage. Multiple arrays, or a larger array of surface seismometers would be required to cover the whole field. CO_2 injection in a vertical well 50 m from the monitoring well began 6 mo after array installation. Several horizontal production wells are sited to the northwest (NW) and southeast (SE) of the injection point.

Fig. 4 shows the rates of water and CO_2 injection through the vertical injection well, and the resulting rates of microseismicity. A small number of events were recorded before injection—this can be considered to be the background rate of microseismicity. Several events occurred during the initial stages of injection, and the seismicity rate increased when the injection rate was increased in June 2004. However, from 2006 onward, almost no seismicity was detected until 2010. A total of ~100 events were recorded between 2003 and 2010. In September 2010, the injection

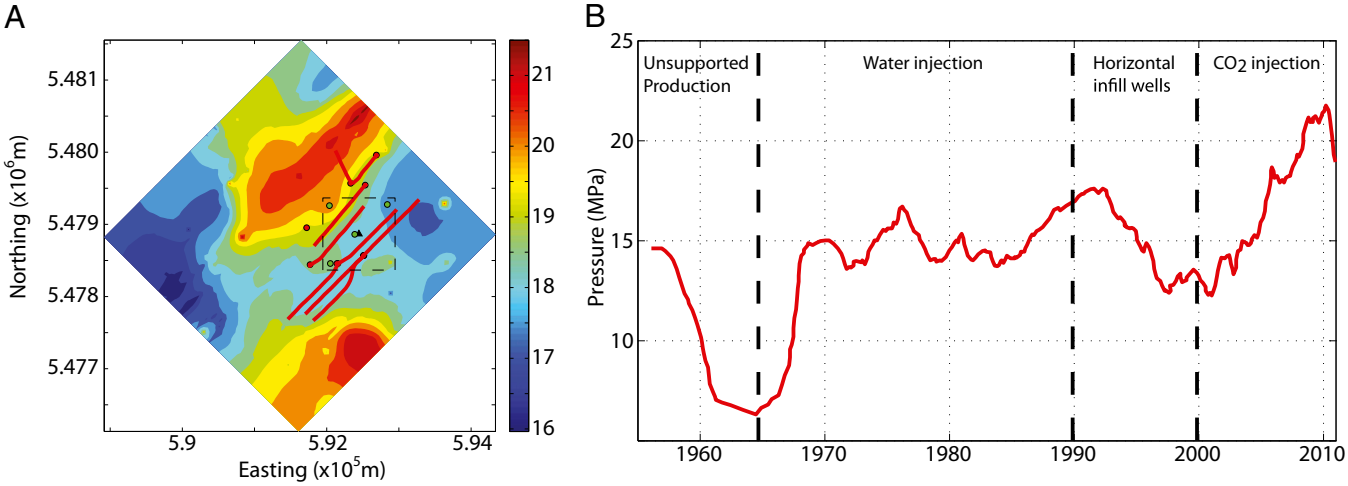

Fig. 3. Modeled pore pressures in the Weyburn reservoir. *A* shows a map of pore pressures on January 1, 2010 (in megapascals). A subset of horizontal production wells (red lines) and vertical injection wells (green dots) in the microseismic monitoring area (dashed square) are shown. *B* shows average field pressures over the history of the field.

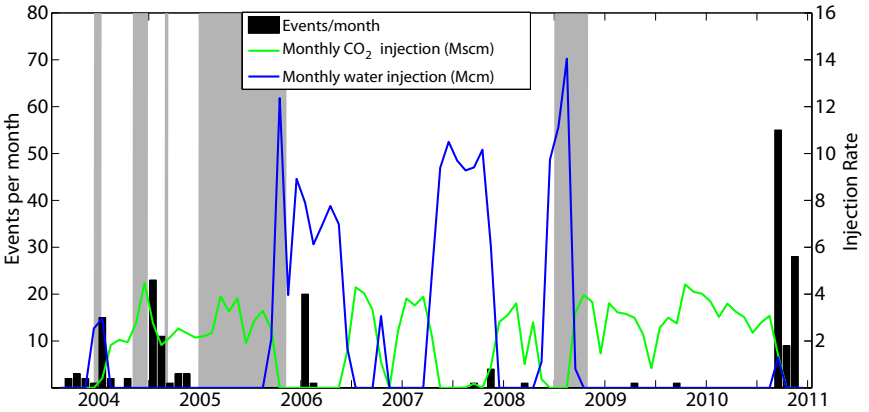

Fig. 4. Rates of CO_2 and water injection in the well adjacent to the microseismic monitoring array, and the resulting rates of microseismicity. The shaded areas indicate periods when the monitoring array was inoperative.

well was shut in. During the month after shut-in, a further 92 events were recorded.

Event hypocenter locations are plotted in Fig. 5. The loci of microseismicity during CO_2 injection (green, blue, and yellow dots) are centered on the production wells to the NW and SE of the injection well. Although the events occurred around the reservoir interval, a significant number appear to be located in the overburden slightly above the reservoir (Fig. 5*B*). The event hypocenters are perhaps surprising, given that conventional injection-induced seismicity theory suggests that seismicity should be induced at the injection points, where elevated pore pressures lead to reduced effective normal stresses. The events above the reservoir may also be of concern if they indicate fracturing and hydraulic communication into the overburden.

Conversely, the events that occurred after shut-in of the injection well were found to cluster around the injection point (red dots). Again, this pattern of seismicity is not intuitive, where it might be expected that the pressure decrease after shut-in of the injection well would reduce the likelihood of seismicity in this area.

The complex pressure history of the reservoir must be taken into account when interpreting these apparently counterintuitive patterns of microseismicity. Verdon et al. (48) constructed a numerical simulation of the deformation at Weyburn, accounting for initial depletion followed by reinjection, and production through horizontal wells. They assessed the likelihood of microseismicity by considering the development of both shear and normal stresses via a fracture potential term (49), finding that, although normal stresses are reduced at the injection point, so are the shear stresses. This means that the potential for seismicity is not increased by injection. Indeed, the shear stress reduction slightly exceeded the effect of normal stress reduction, causing

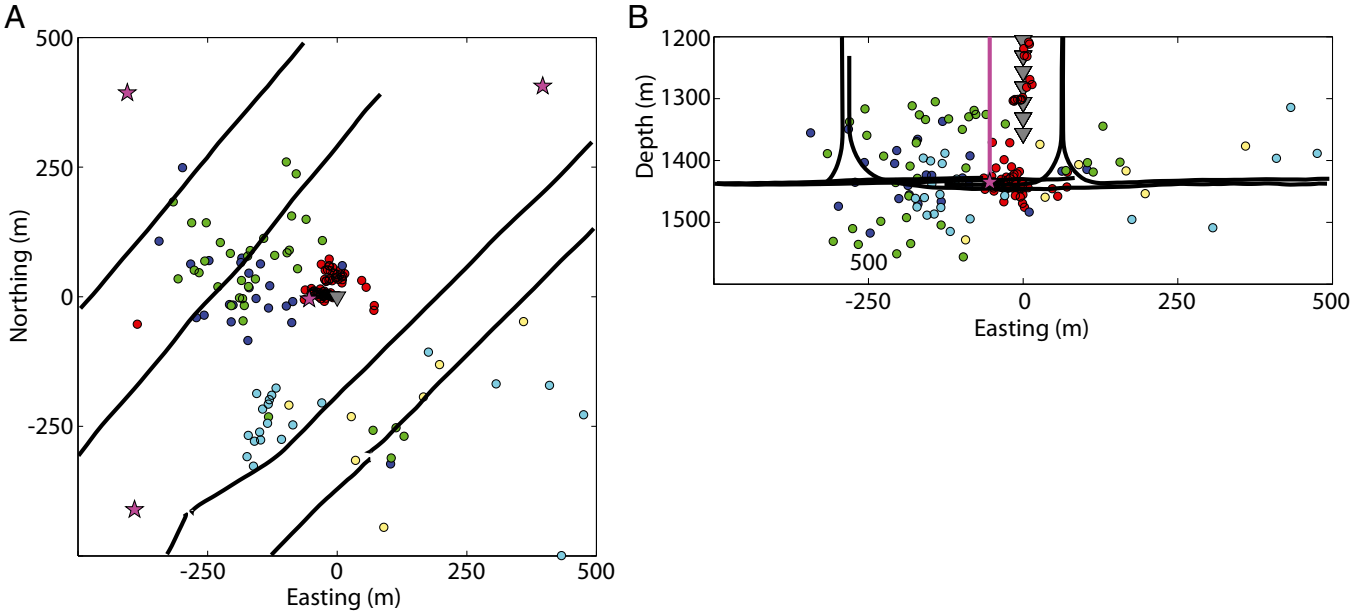

Fig. 5. Locations of microseismic events recorded at Weyburn between 2003 and 2010, in map view (*A*) and projected onto an E–W cross-section (*B*). In *A*, the locations of the injection wells (stars), monitoring well (gray triangle), and horizontal producing wells (black lines) are marked. In *B*, the geophones (gray triangles), injection wells (purple lines), and production wells (black lines) are marked. The reservoir interval can be identified from the depth of the lateral wells. Events are colored by occurrence time: before CO_2 injection (yellow), during the initial injection stages (dark blue), during a period of elevated injection, Summer 2004 (green), during the second phase of monitoring, 2005–2006 (light blue), and after injection well shut-in September 2010 (red). The location of the microseismic monitoring area with respect to the oilfield is shown by the dashed square in Fig. 3*A*.

a slight decrease in the seismicity potential. Conversely, at the production wells, although normal stresses do increase, the shear stresses increase dominated, creating a significant increase in seismicity potential at the producing wells.

Notably, Verdon et al. (48) found that stress changes induced by deformation of the reservoir are transferred into the overburden, leading to an increase in shear stress above the production wells. It is likely that it is this stress transfer into the overburden that accounts for the events located in the overburden above the producing wells. These events are unlikely to have been caused by a hydraulic connection into the overburden—if this were the case, then seismicity would be most likely to occur above the injection well, where pressures are highest and most of the buoyant CO_2 is situated.

All of the recorded microseismicity is located within 200 m of the top of the reservoir, implying that the induced deformation has not created pathways for fluid flow beyond the containment complex. The deformation that has been induced in the overburden is caused by stress transfer rather than a hydraulic connection. This implies that the current deformation does not pose a direct risk to storage security (although continued monitoring is recommended). This is in line with other geophysical and geochemical observations that indicate that the sealing units at Weyburn are performing satisfactorily (50, 51). However, the fact that flexural stress changes are able to trigger microseismic events in the overburden implies that small discontinuities are present that are close to failure criteria. Had larger faults been present in these areas, they too may have been close to failure, presenting an increased risk of both inducing felt seismic events and to caprock integrity. This serves to emphasize the importance of geophysical fault identification and characterization before CO_2 injection.

In Salah

At In Salah, CO_2 present in the natural gas produced from several fields is stripped and injected into the water leg of the Krechba gas reservoir. Along with gas production from the reservoir, CO_2 injection was initiated in 2004, and to date 3.85 million tons have been stored. The target reservoir consists of a 20-m–thick, fractured sandstone at depths of 1,850–1,950 m, with porosity of 13–20% and permeability of ~1 md (11). The sealing units at In Salah consist of a 950-m–thick sequence of mixed mudstones. To improve injectivity into the relatively low-permeability sand, CO_2 is injected through three horizontal wells (KB-501, KB-502, and KB-503) (Fig. 6) of 1- to 1.5-km length, orientated parallel to the direction of minimum horizontal stress (NE–SW), with the intention of maximizing the additional per-

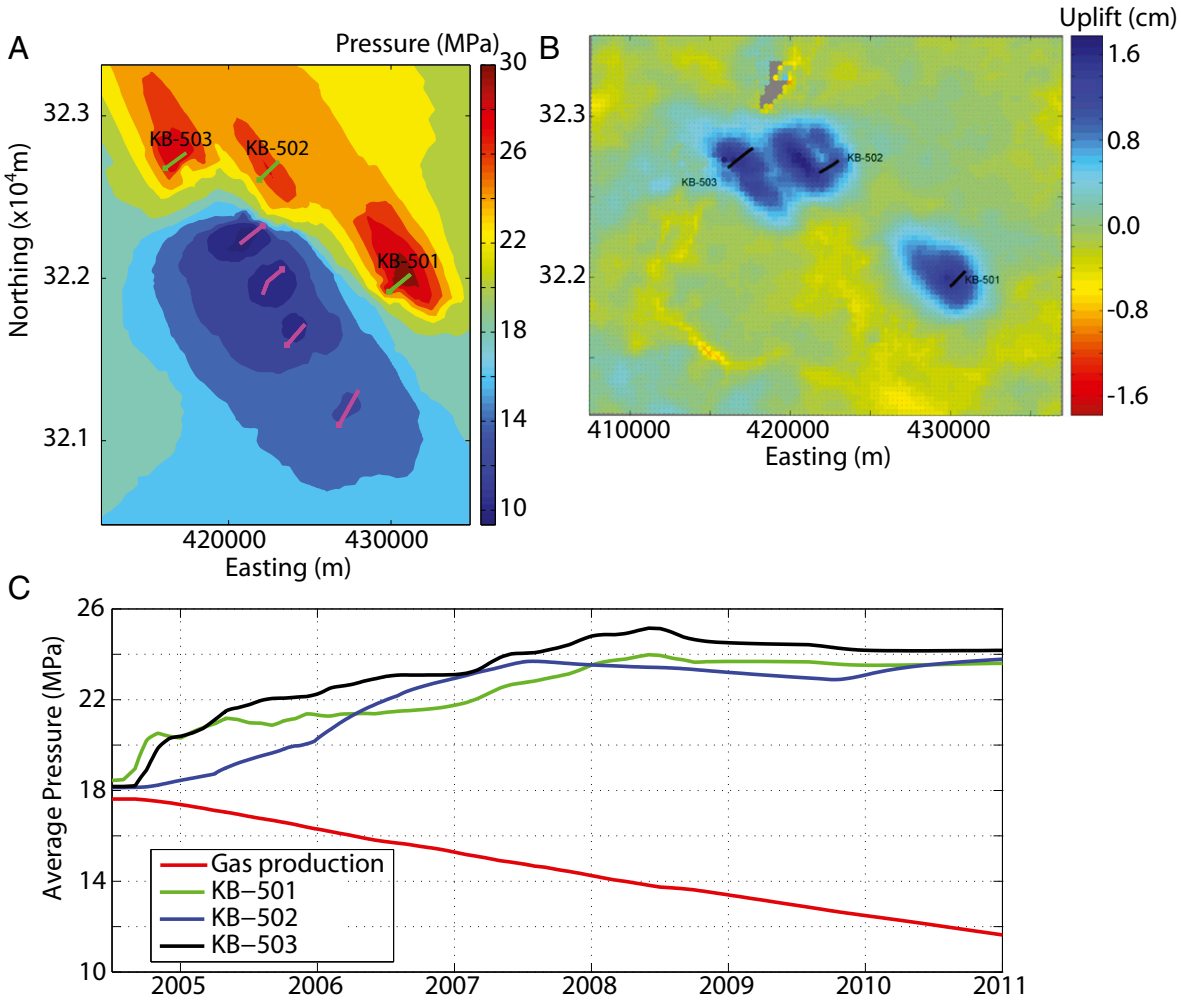

Fig. 6. Modeled pore pressures and geomechanical deformation at In Salah. *A* shows a map of pore pressures after 3 y of injection, whereas *C* shows modeled pressures at the three injection wells and in the producing part of the reservoir. *B* shows surface uplift as measured by InSAR (courtesy of Tele-Rilevamento Europa).

meability provided by the dominant fracture set (which strikes NW–SE) to improve injectivity.

Although CO_2 is injected into the water leg of a producing gas reservoir, there is little apparent pressure communication between the producing and injecting parts of the reservoir, which would serve to moderate the pressure increases during injection. Bissell et al. (16) developed a reservoir flow simulation for In Salah, which attempted to match both CO_2 injection rates/pressures and observed ground displacement. Modeled pore pressures at the injection points have increased substantially from initial conditions of ~18 to ~30 MPa, while reducing to ~10 MPa along the producing crest of the reservoir. Fig. 6*C* shows the maximum, mean, and minimum pressures across the field based on the history-matched flow simulation of Bissell et al. (16), whereas Fig. 6*A* shows a map of modeled pressures in the reservoir.

Initial indications of geomechanical deformation at In Salah were provided by InSAR measurements of surface uplift (52), which showed displacements of ~1 cm/y centered on each of the three injection wells. Subsequent InSAR studies have further constrained the magnitude and extent of this uplift (53), indicating surface uplift of ~2 cm over 5 y of injection. Fig. 6*B* shows the measured uplift after 3 y of injection. The bilobate pattern of uplift above well KB-502 is of particular interest. Numerical inversion of the observed uplift for geomechanical processes at depth have revealed that the bilobate pattern is best explained by the presence of a fault or fracture zone extending from the reservoir 100–200 m into the overburden (29, 54). A similar, albeit smaller, feature was identified at well KB-501 as well. The modeled fracture zone inferred from inversion of the surface uplift at KB-502 matches with a linear feature identified in 3D reflection seismic data (55). It is important to note that, although the development or reactivation of this fracture zone is interesting from a scientific perspective, and potentially of relevance to future CCS operations, the fracture zone of 100–200 m remains well within the 950-m–thick sealing caprock, so does not at present pose a risk to the integrity of the storage system.

To further characterize the deformation occurring at KB-502, a microseismic monitoring array was installed in 2009. The initial array consisted of six three-component geophones in a vertical borehole above the KB-502 injection point, extending to 500-m depth (56). Unfortunately, technical problems have meant that only one of the six geophones has provided useable data. With only one geophone, triangulation for accurate event locations is not possible. Nevertheless, the recorded data have provided further constraint on the geomechanical deformation induced by injection in KB-502.

Even a single geophone allows the rate of microseismic activity to be determined. Fig. 7*A* shows the number of microseismic events manually identified during the first 4 mo of 2010. A total of 700 events were identified, with a maximum of 35 events in 1 d. Using an automated algorithm, Oye et al. (57) were able to detect more than 1,000 events in the whole of 2010. This represents a significantly larger amount of microseismicity compared with the 100 events identified during 6 y of monitoring at Weyburn.

With only a single functioning geophone, it is not possible to accurately locate event hypocenters. Nevertheless, the recorded microseismic data still provides much useful information. In particular, we can examine whether the microseismic data are consistent with the inferences about geomechanical deformation drawn from InSAR and seismic data. Some constraint on event location can be gleaned from the differential arrival times of event P and S waves, which provide an indication of the distance from source to geophone, and the azimuth and inclination of P-wave particle motion, which provide an indication of the direction of the source from the geophone. This information is plotted for the identified events in Fig. 7*B*.

The first notable feature of Fig. 7*B* is the clustering of events: we identify two clusters, one with $t_S - t_P$ of ~0.65 s and near-vertical incidence angles, and a second with $t_S - t_P$ of ~1 s, incidence angles from 18–25°, and azimuths of ~300°. This apparent clustering of events may represent the reactivation of a specific structural feature, in contrast to the "cloud-like" distribution of events at Weyburn that implies more distributed deformation. This is consistent with the inferences about the reactivation of a discrete fracture zone drawn from InSAR and seismic monitoring at In Salah.

The distance from source to geophone can be determined from differential $t_S - t_P$ arrival times, although there is a certain degree of velocity-model dependence (as is true of all microseismic event location methods). Knowledge of source–geophone distance can be used to constrain the event location to a hemisphere (or "pudding bowl")-shaped locus centered on the geophone. If the main cluster of events have occurred directly below the geophone, as suggested by the subvertical incidence angles, a differential

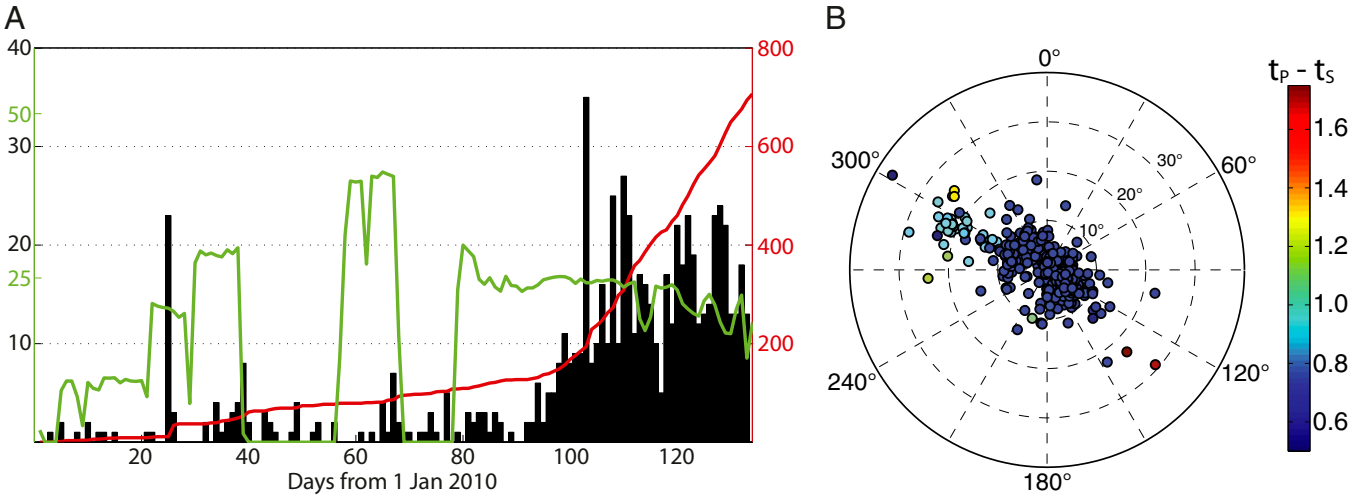

Fig. 7. Microseismicity at In Salah. *A* shows rate of microseismicity (per day, black) and cumulative number of events (red) during the first 4 mo of 2010. Also shown (green) is the CO_2 injection rate (in million standard cubic feet per day). *B* shows event arrival angles on a polar projection, colored by differential S-wave – P-wave arrival times.

arrival time of $t_S - t_P = 0.65$ s roughly corresponds to the depth of the reservoir. This corroborates the presence of a fracture zone at and 100–200 m above the reservoir as inferred from InSAR and seismic reflection data (Fig. S1).

Determination of the depth of secondary cluster, with higher incidence angles and larger differential arrival times, will be more prone to velocity model effects, due to ray bending through a layered model. As such, we cannot constrain whether they originate above, at, or below the reservoir. Nevertheless, the arrival azimuths of ~300° for these events is reasonably consistent with the strike of the feature identified by InSAR and seismic monitoring.

Overall, despite technical issues that have severely limited the quality of the microseismic data, preventing the accurate location of event hypocenters, our observations are consistent with inferences drawn from InSAR and seismic monitoring that CO_2 injection at KB-502 has stimulated a fracture zone extending 100–200 m into the overburden. Crucially, microseismic data have the potential to provide an early warning if this style of deformation were to change. For instance, if this zone of deformation were to begin extending further into the overburden, we would expect to see a reduction in $t_S - t_P$ times as event sources became shallower.

Discussion

The Geomechanical Response to CO2 Injection. Our comparisons between the megatonne storage sites show the significance of geomechanical deformation with respect to CO_2 storage integrity. In particular, they have shown the importance of the pressure increase induced by CO_2 injection in controlling the strength of the geomechanical response. At Sleipner, where the target aquifer is very large, pressure increases during injection are minimal, so very little geomechanical deformation is created. At Weyburn, ongoing enhanced oil recovery serves to mitigate the pressure increase. However, the long history of the field, combined with the pore pressure variations across the field, lead to complex, sometimes nonintuitive patterns of deformation. Nevertheless, the deformation does not appear to compromise storage integrity—in fact, microseismicity is generally associated with lower pore pressures at the production wells.

At In Salah, although injection is nominally into a producing gas reservoir, it is in fact into the water leg of the reservoir, which does not appear to have good pressure communication with the producing parts. Therefore, the natural gas extraction does not compensate for the injection, and pore pressures have increased significantly. This in turn has lead to substantial geomechanical deformation that has uplifted the surface by 2 cm, generated thousands of microseismic events, and appears to have reactivated a fracture network extending from the reservoir 100–200 m into the overburden. At In Salah, the caprock complex is 950 m thick, meaning that fractures propagating a small distance into the overburden do not pose a risk to storage security. However, deformation at In Salah has provided an important learning experience, and similar deformation would perhaps pose a much greater risk to a reservoir with a thinner caprock sequence.

Given the influence of pore pressure on geomechanical deformation, options for pressure management must be considered. Experience shows us that, if we can find large aquifers with good flow properties, like the Utsira Sand, then pore pressure increases will be minimal. However, it is unlikely that all CCS sites will be as effective as Sleipner. Alternatively, mature oilfields may be sought where the postproduction pressures are significantly below initial conditions. However, it is unlikely that such cases will have sufficient volume for large-scale CCS on longer timescales. Furthermore, stress hysteresis means that restoring the original pore pressures may not restore the initial stress conditions (58). Such geomechanical effects must be accounted for during site selection.

If pore pressure increases become problematic, one solution is to remove the in situ fluid from the reservoir. However, this may simply move the problem down the line, as any extracted water must either be treated or re-stored in an alternative reservoir. Moreover, this may significantly add to the costs of storage. Additionally, experience at Weyburn shows that, where both injection and production occur simultaneously, the geomechanical response can be more complicated and sometimes nonintuitive. These effects will need to be accounted for on a site-specific basis via numerical geomechanical modeling.

Geomechanical Monitoring Methods. Comparisons of deformation at these 3-Mt storage sites has afforded us an insight into the relative merits of the various methods for monitoring geomechanical deformation. At Sleipner, time-lapse seismics have been used to determine the pressure change in the reservoir (45), although in this case the null result—that pressure increases were negligible—was found. In producing oilfields, changes in the travel time above the reservoir have been used to infer stress transfer into the overburden (31, 32). Similarly, azimuthal variations in seismic attributes (59) and/or S-wave splitting (60) have been used to image the creation and reactivation of fracture networks due to reservoir deformation.

The use of time-lapse reflection seismics to image stress changes in the subsurface remains an immature technology. However, it is probable that time-lapse seismics will be deployed at the majority of future CCS sites to image fluid substitution effects. With this in mind, it is sensible to consider how time-lapse seismics can be used to image geomechanical as well as fluid saturation changes during CO_2 injection.

Satellite-based InSAR monitoring can reveal surface displacement with millimeter accuracy, and is a very cheap method to determine whether CO_2 injection has produced surface uplift. The rocky, desert conditions at In Salah provided ideal conditions for InSAR monitoring, producing striking images of surface displacement (52) that could be inverted for deformation at reservoir depths (29). Where conditions are suited for InSAR, it should be considered simply because it is so cost effective. However, it should first be noted that InSAR cannot be used for offshore reservoirs, which comprise a significant number of putative future storage sites. Similarly, InSAR monitoring can be more challenging in heavily vegetated and/or farmed areas.

Preexisting permanent structures (buildings, pylons, etc.) or purpose-built reflectors can be used in such scenarios. However, it is worth asking how many preexisting or purpose-built reflectors would be necessary to provide a useful image of the surface uplift? Given say 50 or 100 discrete reflection points, rather than the full and continuous ground coverage that was achieved at In Salah, would Fig. 6*B* be as striking or as useful for inverting for deformation at depth. One can easily imagine, for instance, that the low at the center of the bilobate pattern above well KB-502 could have been missed had no reflection point been present through this zone, without which the true nature of the bilobate pattern of uplift, necessary to identify the presence of a fracture zone, may not have been distinguished.

Microseismic monitoring has been installed at both the Weyburn and In Salah reservoirs. In both, it has been effective at characterizing the geomechanical deformation induced by injection: at Weyburn, the events located around and above the production wells have shown the nonintuitive deformation produced by injection into a mature oilfield with a long and complex history. Only one downhole array was installed, which has proved effective for imaging the events that have occurred in this part of the reservoir. However, the effective range of such monitoring wells is typically 500–1,000 m, meaning that it only covers a very small portion of the total CO_2 injection footprint. Many more arrays would have to be installed to comprehensively cover the whole field, which would considerably increase the cost of monitoring. An alternative to

downhole arrays that might be attractive in some cases is to install dense arrays of surface geophones, where beam-forming and migration techniques are then used to locate microseismic events (40).

At In Salah, the geophones were installed with the principal aim of identifying whether microseismicity was occurring, rather than to accurately locate events. The array has shown the large number of events produced as pore pressures are elevated above initial conditions. Smaller, sparse surface arrays will be significantly cheaper than downhole or dense surface arrays, and can prove useful in characterizing whether seismogenic deformation is occurring, even if event locations are not as accurate. In our opinion, some form of microseismic monitoring should be conducted above any site where appreciable increases in pore pressure are expected during CO_2 injection. Crucially, monitoring arrays should be installed before injection, so that background, baseline rates of seismicity can be determined.

Collectively, our comparisons have shown the importance of characterizing the geomechanical properties of a potential target reservoir before CO_2 injection. This may include the identification of any preexisting faults and fracture networks in the reservoir and overburden, the in situ stress conditions, the characteristics of any background microseismicity, as well as laboratory measurements to determine the mechanical properties of reservoir and overburden rocks. Effective characterization of the reservoir is necessary to produce accurate numerical models that simulate injection-induced seismicity. Site-specific geomechanical characterizations have been performed for a number of sites, including the Gippsland (61) and Otway (62) Basins, a sedimentary basin in Japan (63), Teapot Dome, Wyoming (64), and The Rose Run Sandstone, Ohio (65), Weyburn (66), and the Dogger Carbonate, Paris Basin (67).

If a target reservoir has pore volume and permeability characteristics such that significant pore pressure increases during injection are likely, we recommend that geomechanical deformation be monitored. InSAR monitoring has proven to be an excellent tool to image surface uplift produced by injection. However, the effectiveness of InSAR may be limited to certain environments. Microseismic monitoring has proved to be an effective tool to monitor deformation at Weyburn and In Salah, and in a range of other settings, and we recommend that microseismic monitoring of some description is deployed at any CCS site that is likely to be prone to geomechanical deformation.

ACKNOWLEDGMENTS. This paper relies on data from each of the CCS sites discussed. We are grateful to the operators of the Sleipner, Weyburn, and In Salah fields (Statoil, BP, Sonatrach, Cenovus) and associated research bodies (Petroleum Technology Research Center, Canada, and the In Salah Joint Industry Project) for access to the data on which this paper is based. We also acknowledge Volker Oye and group at Norwegian Seismic Array (NORSAR) for their work on the In Salah microseismic data, and Mark Zoback for his helpful comments on the paper. J.P.V. is a Natural Environment Research Council Early-Career Research Fellow (Grant NE/I021497/1). This research was conducted under the auspices of the Bristol CO_2 Group.

1. Haszeldine RS (2009) Carbon capture and storage: How green can black be? *Science* 325(5948):1647–1652.
2. Bickle MJ (2009) Geological carbon storage. *Nat Geosci* 2:815–818.
3. Pacala S, Socolow R (2004) Stabilization wedges: Solving the climate problem for the next 50 years with current technologies. *Science* 305(5686):968–972.
4. Zoback MD, Gorelick SM (2012) Earthquake triggering and large-scale geologic storage of carbon dioxide. *Proc Natl Acad Sci USA* 109(26):10164–10168.
5. Vangkilde-Pedersen T, et al. (2009) Assessing European capacity for geological storage of carbon dioxide—the EU GeoCapacity project. *Energy Procedia* 1:2663–2670.
6. Crow W, Carey JW, Gasda S, Williams DB, Celia M (2010) Wellbore integrity analysis of a natrual CO_2 producer. *Int J Greenh Gas Control* 4:186–197.
7. Rochelle CA, Czernichowski-Lauriol I, Milodowski AE (2004) The impact of chemical reactions of CO_2 storage in geological formations: A brief review. *Geological Storage of Carbon Dioxide*, Geological Society of London Special Publication, eds Baines SJ, Worden RH (Geological Society of London, London), pp 87–106.
8. Economides MJ, Ehlig-Economides CA (2009) *Sequestering Carbon Dioxide in a Closed Underground Volume* (Society of Petroleum Engineers, Richardson, TX), SPE 124430.
9. Arts RJ, Chadwick RA, Eiken O, Thibeau S, Nooner S (2008) Ten years' experience of monitoring CO_2 injection in the Utsira Sand at Sleipner, offshore Norway. *First Break* 26:65–72.
10. Wilson M, et al. (2004) *IEA GHG Weyburn CO_2 Monitoring and Storage Project Summary Report 2000–2004* (Petroleum Technology Research Centre, Regina, SK, Canada).
11. Mathieson A, et al. (2010) CO_2 sequestration monitoring and verification technologies applied at Krechba, Algeria. *Leading Edge (Tulsa Okla)* 29:216–222.
12. Rodosta T, et al. (2011) U.S. Department of Energy's Regional Carbon Sequestration Partnership Initiative: Update on validation and development phases. *Energy Procedia* 4:3457–3464.
13. Terzaghi K (1943) *Theoretical Soil Mechanics* (Wiley, New York).
14. Segura JM, et al. (2011) Reservoir stress path characterization and its implications for fluid-flow production simulations. *Petrol Geosci* 17:335–344.
15. Armitage PJ, et al. (2011) Experimental measurement of, and controls on, permeability and permeability anisotropy of caprocks from the CO_2 storage project at the Krechba Field, Algeria. *J Geophys Res* 116:B12208.
16. Bissell RC, et al. (2011) A full field simulation of the In Salah gas production and CO_2 storage project using a coupled geomechanical and thermal fluid flow simulator. *Energy Procedia* 4:3290–3297.
17. Zoback MD, Zinke JC (2002) Production-induced normal faulting in the Valhall and Ekofisk oil fields. *Pure Appl Geophys* 159:403–420.
18. Løseth H, Gading M, Wensaas L (2009) Hydrocarbon leakage interpreted on seismic data. *Mar Pet Geol* 26:1304–1319.
19. Evans DJ (2009) A review of underground fuel storage events and putting risk into perspective with other areas of the energy supply chain. *Geol Soc Lond Spec Publ* 313: 173–216.
20. Evans DM (1966) The Denver Area earthquakes and The Rocky Mountain Arsenal disposal well. *Mt Geol* 3:23–36.
21. Nicholson C, Wesson RL (1992) Triggered earthquakes and deep well activities. *Pure Appl Geophys* 139:561–578.
22. National Academy of Sciences (2012) *Induced Seismicity Potential in Energy Technologies* (The National Academies Press, Washington, DC).
23. Van Noorden R (2010) Carbon sequestration: Buried trouble. *Nature* 463(7283): 871–873.
24. Dusseault MB, Bruno MS, Barrera J (1998) *Casing Shear: Causes, Cases, Cures* (Society of Petroleum Engineers, Richardson, TX), SPE 48864.
25. Nagel NB (2001) Compaction and subsidence issues within the petroleum industry: From Wilmington to Ekofisk and beyond. *Phys Chem Earth Part A Solid Earth Geod* 26:3–14.
26. Biggs J, Anthony EY, Ebinger CJ (2009) Multiple inflation and deflation events at Kenyan volcanoes. East African Rift. *Geology* 37:979–982.
27. Vasco D, Karasaki K, Doughty C (2000) Using surface deformation to image reservoir dynamics. *Geophysics* 65:132–147.
28. Gebauer A, Jahr T, Jentzsch G (2007) Recording and interpretation/analysis of tilt signals with five ASKANIA borehole tiltmeters at the KTB. *Rev Sci Instrum* 78(5): 054501.
29. Vasco DW, et al. (2010) Satellite-based measurements of surface deformation reveal fluid flow associated with the geological storage of carbon dioxide. *Geophys Res Lett* 37:L03303.
30. Nur AM, Simmons G (1969) The effect of saturation on velocity in low porosity rocks. *Earth Planet Sci Lett* 7:183–193.
31. Hatchell P, Bourne S (2005) Rocks under strain: Strain-induced time-lapse time shifts are observed for depleting reservoirs. *Leading Edge (Tulsa Okla)* 24:1222–1225.
32. Staples R, Ita J, Burrell R, Nash R (2007) Monitoring pressure depletion and improving geomechanical models of the Shearwater field using 4D seismic. *Leading Edge (Tulsa Okla)* 26:636–642.
33. Sarkar D, Bakulin A, Kranz RL (2003) Anisotropic inversion of seismic data for stressed media: Theory and a physical modeling study on Berea Sandstone. *Geophysics* 68: 690–704.
34. Herwanger J, Horne S (2009) Linking reservoir geomechanics and time-lapse seismics: Predicting anisotropic velocity changes and seismic attributes. *Geophysics* 74: W13–W33.
35. Maxwell SC (2010) Microseismic: Growth born from success. *Leading Edge (Tulsa Okla)* 29:338–343.
36. Dyer BC, Cowles RHJJF, Barkved O, Folstad PG (1999) Microseismic survey of a North Sea reservoir. *World Oil* 220:74–78.
37. Jones RH, Raymer D, Mueller G, Rynja H, Maron K (2004) Microseismic monitoring of the Yibal Oilfield. *66th EAGE Annual Meeting, Expanded Abstracts* (European Association of Geoscientists and Engineers, Houten, The Netherlands), A007.
38. De Meersman K, Kendall J-M, Van der Baan M (2009) The 1998 Valhall microseismic data set: An integrated study of relocated sources, seismic multiplets and S-wave splitting. *Geophysics* 74(5):B183–B195.
39. Maxwell SC, Rutledge J, Jones R, Fehler M (2010) Petroleum reservoir characterization using downhole microseismic monitoring. *Geophysics* 75:A129–A137.
40. Chambers K, Kendall J-M, Brandsberg-Dahl S, Rueda J (2010) Testing the ability of surface arrays to monitor microseismic activity. *Geophys Prospect* 58:821–830.
41. Teanby NA, Kendall J-M, Jones RH, Barkved O (2004) Stress-induced temporal variations in seismic anisotropy observed in microseismic data. *Geophys J Int* 156: 459–466.
42. Verdon JP, Kendall J-M (2011) Detection of multiple fracture sets using observations of shear-wave splitting in microseismic data. *Geophys Prospect* 59:593–608.

43. Verdon JP, Kendall J-M, Maxwell SC (2010) A comparison of passive seismic monitoring of fracture stimulation due to water versus CO_2 injection. *Geophysics* 75(3):MA1–MA7.
44. Chadwick RA, Holloway S, Brook M, Kirby G (2004) The case for underground CO_2 sequestration in northern Europe. *Geological Storage of Carbon Dioxide*, Geological Society of London Special Publication, eds Baines SJ, Worden RH (Geological Society of London, London), pp 17–28.
45. Chadwick RA, Williams GA, Williams JDO, Noy DJ (2012) Measuring pressure performance of a large saline aquifer during industrial-scale CO_2 injection: The Utsira Sand, Norwegian North Sea. *Int J Greenh Gas Control* 10:374–388.
46. Eiken O, Tøndel R (2005) Sensitvity of time-lapse seismic data to pore pressure changes: Is quantification possible? *Leading Edge (Tulsa Okla)* 24:1250–1254.
47. Maxwell SC, White DJ, Fabriol H (2004) Passive seismic imaging of CO_2 sequestration at Weyburn. *SEG Expanded Abstracts* 23:568–571.
48. Verdon JP, Kendall J-M, White DJ, Angus DA (2011) Linking microseismic event locations with geomechanical models to minimise the risks of storing CO_2 in geological formations. *Earth Planet Sci Lett* 305:143–152.
49. Connolly PT, Cosgrove JW (1999) Prediction of fracture induced permeability and fluid flow in the crust using experimental stress data. *Bulletin of the AAPG* 85(5): 757–777.
50. Gilfillan SMV, Haszeldine RS (2011) Report on noble gas, carbon stable isotope and HCO^-_3 measurements from the Kerr Quarter and surrounding area, Goodwater, Saskatchewan. *The Kerr Investigation: Final Report, Findings of the Investigation into the Impact of CO_2 on the Kerr Property*, ed Sherk GW (Petroleum Technology Research Centre, Regina, SK, Canada), pp 77–102.
51. White DJ, et al. (2011) Geophysical monitoring of the Weyburn CO_2 flood: Results during 10 years of injection. *Energy Procedia* 4:3628–3635.
52. Onuma T, Ohkawa S (2009) Detection of surface deformation related with CO_2 injection by DInSAR at In Salah, Algeria. *Energy Procedia* 1:2177–2184.
53. Vasco DW, Ferretti A, Novali F (2008) Reservoir monitoring and characterization using satellite geodetic data: Interferometric synthetic aperture radar observations from the Krechba field, Algeria. *Geophysics* 73(6):WA113–WA122.
54. Morris JP, Hao Y, Foxall W, McNab W (2011) A study of injection-induced mechanical deformation at the In Salah CO_2 storage project. *Int J Greenh Gas Control* 5:270–280.
55. Rutqvist J (2012) The geomechanics of CO_2 storage in deep sedimentary formations. *Geotech Geol Eng* 30:525–551.
56. Mathieson A, Midgely J, Wright I, Saoula N, Ringrose P (2011) In Salah CO_2 storage JIP: CO_2 sequestration monitoring and verification technologies applied at Krechba, Algeria. *Energy Procedia* 4:3596–3603.
57. Oye V, et al. (2012) Monitoring of the Salah CO_2 storage site (Krechba) using microseismic data analysis. *3rd EAGE CO_2 Geological Storage Workshop, Expanded Abstracts* (European Association of Geoscientists and Engineers, Houten,The Netherlands).
58. Santarelli F, Tronvoll J, Svennekjaer M, Skeie H, Henriksen R, Bratli R (1998) *Reservoir Stress Path: The Depletion and the Rebound* (Society of Petroleum Engineers, Richardson, TX), SPE 47350.
59. Duxbury A, et al. (2012) Fracture mapping using seismic amplitude variation with offset and azimuth analysis at the Weyburn CO_2 storage site. *Geophysics* 77(17-N):28.
60. Olofsson B, Probert T, Kommedal JH, Barkved O (2003) Azimuthal anisotropy from the Valhall 4C 3D survey. *Leading Edge (Tulsa Okla)* 22:1228–1235.
61. van Ruth PJ, Nelson EJ, Hillis RR (2006) Fault reactivation potential during CO_2 injection in the Gippsland Basin, Australia. *Explor Geophys* 37:50–59.
62. Vidal-Gilbert S, et al. (2010) Geomechanical analysis of the Naylor Field, Otway Basin, Australia: Implications for CO_2 injection and storage. *Int J Greenh Gas Control* 4: 827–839.
63. Li Q, Wu Z, Li X, Murakami Y (2006) Site geomechanics analysis of CO_2 geological sequestration. *10th IAEG International Congress: Engineering Geology for Tomorrow's Cities* (Geological Society of London, London), Paper 129.
64. Chiaramonte L (2008) Geomechanical characterization and reservoir simulation of a CO_2 sequestration project in a mature oil field, Teapot Dome, Wy. PhD thesis (Stanford University, Stanford, CA).
65. Lucier A, Zoback M, Gupta N, Ramakrishnan TS (2006) Geomechanical aspects of CO_2 sequestration in a deep saline reservoir in the Ohio River Valley region. *Environ Geosci* 13:85–103.
66. Jimenez Gomez JA (2006) Geomechanical performance assessment of CO_2—EOR geological storage projects. PhD thesis (University of Alberta, Edmonton, AB, Canada).
67. Vidal-Gilbert S, Nauroy J-F, Brosse E (2009) 3D geomechanical modelling for CO_2 geologic storage in the Dogger carbonates of the Paris Basin. *Int J Greenh Gas Control* 3:288–299.